Journal of Cellular Physiology

Bax Is Essential for Drp1-Mediated Mitochondrial Fission But Not for Mitochondrial Outer Membrane Permeabilization Caused by Photodynamic Therapy

SHENGNAN WU, FEIFAN ZHOU, ZHENZHEN ZHANG, AND DA XING*

MOE Key Laboratory of Laser Life Science and Institute of Laser Life Science, College of Biophotonics, South China Normal University, Guangzhou, China

Bcl-2 family proteins are critical for the regulation of apoptosis, with the pro-apoptotic members Bax essential for the release of cytochrome *c* from mitochondria in many instances. However, we found that Bax was activated after mitochondrial depolarization and the completion of cytochrome *c* release induced by photodynamic therapy (PDT) with the photosensitizer Photofrin in human lung adenocarcinoma cells (ASTC-a-1). Besides, knockdown of Bax expression by gene silencing had no effect on mitochondrial depolarization and cytochrome *c* release, indicating that Bax makes no contribution to mitochondrial outer membrane permeabilization (MOMP) following PDT. Further study revealed that Bax knockdown only slowed down the speed of cell death induced by PDT, indicating that Bax is not essential for PDT-induced apoptosis. The fact that Bax knockdown totally inhibited the mitochondrial accumulation of dynamin-related protein (Drp1) and Drp1 knockdown attenuated cell apoptosis suggest that Bax can promote PDT-induced apoptosis through promoting Drp1 activation. Besides, Drp1 knockdown also failed to inhibit PDT-induced cell death finally, indicating that Bax-mediated Drp1's mitochondrial translocation is not essential for PDT-induced cell apoptosis. On the other hand, we found that protein kinase Cδ (PKCδ), Bim L and glycogen synthase kinase 3β (GSK3β) were activated upon PDT treatment and might contribute to the activation of Bax under the condition. Taken together, Bax activation is not essential for MOMP but essential for Drp1-mediated mitochondrial fission during the apoptosis caused by Photofrin-PDT.

J. Cell. Physiol. 226: 530–541, 2011. © 2010 Wiley-Liss, Inc.

Apoptosis is a genetically regulated cellular suicide mechanism essential for multicellular organisms to remove damaged or unwanted cells and maintain tissue homeostasis (Taylor et al., 2008). Apoptosis can also be induced by external stimuli and the process includes an ordered cascade of enzymatic events leading to the production of unique morphological and biochemical changes of the cell (Taylor et al., 2008). The most important regulators of the process are proteins of Bcl-2 family members (Chipuk et al., 2010), among which Bax is one of the most important pro-apoptotic members (Chipuk et al., 2010). Bax is located in cytoplasm, while translocates to mitochondria during apoptosis (Chipuk et al., 2010). The membrane insertion and oligomerization of Bax in mitochondria is essential for the release of cytochrome *c* and apoptosis (Chipuk et al., 2010).

Mitochondrial networks have been reported to undergo fission/fragmentation during apoptosis for many years (Desagher and Martinou, 2000). It is widely agreed upon is that fission is a general feature of apoptosis in essentially all cell types and in response to most, if not all, pro-apoptotic stimuli (Frank et al., 2001; Kowaltowski et al., 2002; Arnoult et al., 2005; Sheridan et al., 2008). The opinion of the relationship between apoptosis and fission is divided about whether this phenomenon of fragmentation is simply a consequence of apoptosis or plays a more active role in the process. Some investigators have suggested that mitochondrial fission may promote cytochrome *c* release and therefore act to drive caspase activation during apoptosis (Frank et al., 2001; Youle and Karbowski, 2005). However, other data suggest that apoptosis-associated mitochondrial fission is a consequence rather than a cause of apoptosis and reflects events containing some hitherto unrecognized connection between members of the Bcl-2 family and the mitochondrial morphogenesis machinery (Arnoult et al., 2005; Delivani et al., 2006; Karbowski et al., 2006; Sheridan et al., 2008). Youle and coworkers have published a series of seminal studies demonstrating conclusively that activation of Bax and/or Bak leads rapidly to mitochondrial fragmentation (Frank et al., 2001; Kowaltowski et al., 2002; Karbowski et al., 2004). Furthermore, this event occurs very

Abbreviations: ASTC-a-1, human lung adenocarcinoma cells; ANT, adenine nucleotide translocator; ASK1, apoptosis signal regulating kinase-1; Drp1, dynamin-related protein; DU145, human prostate carcinoma cells; FITC, fluorescein isothiocyanate; FCM, flow cytometry; GSK3β, glycogen synthase kinase 3β; H_2DCFDA, dichlorodihydrofluorescein diacetate; JNK, c-Jun N-terminal kinases; MPT, mitochondrial permeability transition; MOMP, mitochondrial outer membrane permeabilization; PKCδ, protein kinase Cδ; PDT, photodynamic therapy; PARP, ADP-ribose polymerase; Pc 4, phthalocyanine; PI, propidium iodide; RNAi, RNA interference; ROS, reactive oxygen species; Rh123, Rhodamine123; STS, staurosporine; SEM, standard error of the mean; $\Delta\Psi_m$, mitochondrial transmembrane potential.

Contract grant sponsor: National Basic Research Program of China;
Contract grant number: 2010CB732602.
Contract grant sponsor: Program for Changjiang Scholars and Innovative Research Team in University;
Contract grant number: IRT0829.
Contract grant sponsor: National Natural Science Foundation of China;
Contract grant numbers: 30870676, 30870658.

*Correspondence to: Da Xing, MOE Key laboratory of Laser Life Science and Institute of Laser Life Science, College of Biophotonics, South China Normal University, Guangzhou 510631, China.
E-mail: xingda@scnu.edu.cn

Received 23 February 2010; Accepted 27 July 2010

Published online in Wiley Online Library (wileyonlinelibrary.com), 3 August 2010.
DOI: 10.1002/jcp.22362

close in time to MOMP and associated mitochondrial cytochrome *c* release (Arnoult et al., 2005). It is reported that activated Bax frequently decorates mitochondrial scission sites (Karbowski et al., 2004). Mitochondrial fragmentation occurs upstream of caspase activation, as inhibition of caspase activity downstream of Bax/Bak activation fails to block this event (Frank et al., 2001; Sheridan et al., 2008).

Photodynamic therapy (PDT) is a novel treatment for cancer and other abnormal tissues that employs photosensitizer and visible light to produce singlet oxygen and other reactive oxygen species (ROS) that lead to subcellular damage at sites where the photosensitizer accumulates (Triesscheijn et al., 2006). PDT is an efficient inducer of apoptosis, with the initiating reactions dependent on the preferential sites of photosensitizer localization (Oleinick et al., 2002; Agostinis et al., 2004). Many of the commonly used photosensitizers accumulate in the mitochondria, such as Photofrin (Wilson et al., 1997; Rousset et al., 2000; Oleinick et al., 2002). PDT with mitochondrial damaging photosensitizers induces rapid apoptosis through activation of mitochondrial pathway of apoptosis (Oleinick et al., 2002). This includes cytochrome *c* release, caspase activation, poly ADP-ribose polymerase (PARP) cleavage, chromatin condensation and DNA fragmentation (Granville et al., 1998, 1999; He et al., 1998; Kessel and Luo, 1998; Kim et al., 1999; Varnes et al., 1999; Chiu and Oleinick, 2001; Chiu et al., 2001). Bax undergoes a conformational change as well as translocation from cytosol to mitochondria after PDT. Besides, stable overexpression of Bcl-2 can lead to the upregulation of Bax and increased sensitivity to PDT (Carthy et al., 1999; Granville et al., 1999).

Here, we have examined the role of Bax in apoptosis caused by PDT with a mitochondria-targeted photosensitizer Photofrin. Our data show that Bax is essential for Drp1-mediated mitochondrial fission but not for MOMP caused by PDT. Understanding the molecular events that contribute to PDT-induced apoptosis should enable a more rational approach to drug design and therapy.

Materials and Methods

Tumor cell lines

Human lung adenocarcinoma cells (ASTC-a-1) and human prostate carcinoma cells (DU145) were grown on 22-mm culture glasses, in Dulbecco's modified Eagle's medium (DMEM, Life Technologies, Inc., Gaithersburg, MD) supplemented with 15% fetal bovine serum (FBS) (GIBCO Co. LTD, Carlsbad), 50 U/ml penicillin, and 50 μg/ml streptomycin, in 5% CO_2, 95% air, at 37°C in a humidified incubator. In all experiments, 70–85% confluent cultures were used.

Fluorescent probes, reagents, antibodies, and plasmids

The following fluorescent probes (Molecular Probes, Eugene, OR) were used: Dichlorodihydrofluorescein diacetate (H_2DCFDA) (10 μM) to label ROS; MitoTracker Deeper Red 633 (100 nM) to stain mitochondria; Calcein AM (1 μM) to monitor mitochondrial permeability transition (MPT); Rhodamine 123 (Rh123) (5 μM) to indicate mitochondrial transmembrane potential ($\triangle\Psi_m$). The optimal incubation time for each probe was determined experimentally.

Ascorbic acid (250 μM) (Sigma–Aldrich, St. Louis, MO) was used to scavenge ROS. Lithium chloride (LiCl) (20 mM) was used as a GSK3β inhibitor. Staurosporine (STS) (1 μM) was purchased from Sigma–Aldrich. $CoCl_2$ (1 mM) was used to quench the fluorescence of calcein. GÖ6983 (100 nM) was purchased from Merck (Darmstadt, Germany) and used as a protein kinase Cs (PKCs) inhibitor. Lipofectamine™ 2000 reagent (Invitrogen Life Technologies, Inc., Grand Island, NY) was used to transfect plasmid DNAs into cells. Cells were examined 48 h after transfection.

Cytochrome *c* and COX IV monoclonal antibodies were purchased from BD PharMingen (San Diego, CA). Drp1 and β-actin monoclonal antibodies were purchased from Santa Cruz Biotechnology, Inc. (Santa Cruz, CA). Bax monoclonal antibodies were purchased Cell Signaling Technology (Beverly, MA). The plasmid of GFP-Bim L was generated as previously described (Chen et al., 2007).

PDT treatment

Cells were incubated in the dark with Photofrin (2.5 μg/ml) in complete growth medium for 20 h, and then rinsed with PBS before irradiation. For irradiation of single cell, a 633-nm He–Ne laser inside a confocal laser scanning microscope (LSM510-ConfoCor2) (Zeiss, Jena, Germany) was used in PDT. Laser irradiation was performed through the objective lens of the microscope. In this setup, only the cells under observation were irradiated by the laser. A minitype culture chamber with CO_2 supply (Tempcontrol 37-2 digital, Zeiss) was used in order to keep cells under normal culture conditions (37°C, 5% CO_2) during irradiation. For irradiation of multi-cells, cells were irradiated with a He-Ne laser (632.8 nm, HN-1000, Guangzhou, China) in the dark. The cells in selected area were all irradiated for 30 sec with a laser dose of 5 J/cm^2.

Immunofluorescence

Cells grown on 22-mm culture glasses were fixed for 10 min in 4% paraformaldehyde followed by permeabilization with 0.15% Triton X-100 in phosphate-buffered saline for 15 min. The cells were then incubated for 1 h in blocking buffer [2% bovine serum albumin (BSA) in phosphate buffered saline] followed by incubation overnight with either a rabbit monoclonal anti-Drp1 (1:500) antibody. Cells were washed three times for 10 min each in blocking buffer, and then incubated for 2 h with Alexa Fluor 488 dye-conjugated goat anti-rabbit secondary antibodies (Molecular Probes, Eugene, OR). Images were acquired using a LSM510-ConfoCor2 microscope (Zeiss) through a 40× oil fluorescence objective (Carl Zeiss, Inc., Jena, Germany).

Imaging analysis of living cells

In order to image single cells, the confocal microscope was used. Cell images before and after laser irradiation were acquired with a Plan-Neofluar 100×/NA1.3, oil-immersed objective lens. Cells were maintained at 37°C, 5% CO_2 during imaging with the minitype culture chamber with CO_2 supply. The following specific settings were used for light excitation and emissions: MitoTracker Deeper Red 633 (He-Ne laser, Ex. 633 nm, Em. LP 650 nm); 2′,7′-dichlorofluorescin (DCF), calcein, Rh123 and GFP (Ar^+ laser, Ex. 488 nm, Em. BP 500-550 nm); YFP (Ar^+ laser, Ex. 514 nm, Em. BP530-550 nm); CFP (Ar^+ laser, Ex. 458 nm, Em. BP 470–500 nm), and for intracellular measurements, the desired areas were chosen in the confocal image. To quantify the results, the fluorescence emission intensities (concluding the background fluorescence) were obtained with Zeiss Rel 3.2 image processing software (Zeiss).

For Quantitative analysis of fluorescence emission intensity, cells were cultured in 96-well microplates at a density of 4×10^3 cells/well and each well contained 100 μl culture medium. After stained by indicated fluorescent probes (DCF, Rh123, or caclein), the grouped cells were treated by Photofrin-PDT. The interval wells were filled with ink in order to minimize the scattered or reflected light. Immediately after irradiation, fluorescence emission intensity was recorded at indicated time using an Infinite 2000 plate reader (TECAN, Mönnedorf, Switzerland).

Western blotting analysis

Cells were harvested in 300 μl of lysis buffer [50 mM Tris–HCl, pH 8.0, 150 mM NaCl, 50 mM β-glycerol phosphate, 1% Triton X-100,

and 100 mM phenylmethylsulfonyl fluoride (PMSF)]. The resulting lysates were resolved on 4–12% SDS–PAGE and transferred to pure nitrocellulose blotting membranes (BioTrace™ NT, Pall Life Science, Pensacola, FL). The membranes were blocked in TBST (10 mM Tris–HCl, pH 7.4, 150 mM NaCl, 0.1% Tween-20) containing 5% non-fat milk and then probed with different antibodies. Proteins were detected by using Odyssey two-color infrared imaging system (LI-COR, Inc., Lincoln, NE). Mitochondrial and cytosolic fractions were obtained using the Mitochondria Isolation Kit (Cat: KGA 827, KeyGEN, Nanjing, China).

Flow cytometry (FCM)

For FCM analysis, Annexin-V-FITC conjugate, PI dyes, and binding buffer was used as standard reagents. Flow cytometry was performed on a FACScantoII flow cytometer (Becton Dickinson, Mountain View, CA) with excitation at 488 nm. Fluorescent emission of FITC was measured at 515–545 nm and that of DNA-PI complexes at 564–606 nm. Cell debris was excluded from analysis by an appropriate forward light scatter threshold setting. Compensation was used wherever necessary.

RNA interference (RNAi)

The oligonucleotides for short hairpin RNA (shRNA) were purchased from GenePharma (Shanghai, China) for Bim and Genesil Biotechnology Co., Ltd (Wuhan, China) for Bax.

Drp1, Bim, and Bax suppression was accomplished using Drp1 shRNA, Bim shRNA, and Bax shRNA constructs, respectively. The oligonucleotides for shRNA were synthesized as follows: shBim: GCAACCTTCTGATGTAAGTTCTTCAAGAGAGAACTTA-CATCAGAAGGTTGCTT. The sense strand nucleotide sequence for shBax was AACATGGAGCTGCAGAGGATGAdTdT. The target sequence for Drp1 was as follows: TTCAATCCGTGAT-GAGTATGCTTTTCTTC. The shRNA sequences were transfected into cells using Lipofectamine™ 2000 reagent according to the manufacturer's protocol.

Statistics

For the analysis of cytochrome *c* release and Bax translocation, images were analyzed with MATLAB 6.5 software by drawing regions of interest (ROIs) in individual cells for averages and standard error of the mean (SEM) of the intensity of the pixels (punctuate/diffuse) and integrated brightness (total brightness). Unless otherwise indicated, data were analyzed using one-way ANOVA. All results showed in our studies were repeated for at least five times in independent experiments.

Results

Bax is not essential for MOMP caused by PDT

We investigated the correlation of Bax activation with mitochondrial depolarization in ASTC-a-1 cells treated with STS and Photofrin-PDT. Cells were transiently transfected with pCFP-Bax, and after 48-h expression, cells expressing CFP-Bax were labeled with Rh123 to indicate $\triangle\Psi_m$. Cells without any treatment were set as control (Fig. 1A,B). As shown in Figure 1A,C, Bax translocated to mitochondria along with the decrease of Rh123 fluorescence under STS treatment, indicating that Bax activation contributes to mitochondrial depolarization. Photofrin-PDT resulted in a different pattern of Bax activation (Fig. 1A,D): Bax was activated (indicated by the mitochondrial accumulation of Bax) after mitochondrial depolarization (indicated by the disappearance of Rh123 fluorescence).

Western blotting was employed to study the correlation of Bax activation with MOMP in ASTC-a-1 cells treated with STS and Photofrin-PDT. Under STS treatment, the decrease of cytochrome *c* levels was accompanied with the increase of Bax levels in mitochondrial fraction (Fig. 2A), indicating that Bax activation contributes to MOMP. However, the levels of cytochrome *c* in mitochondrial fraction decreased quickly in 40 min post Photofrin-PDT treatment, while the levels of Bax began to increase at about 80 min post the treatment (Fig. 2B), indicating that Bax activation occurs after MOMP.

To explore the role of the Bax on mitochondrial pro-apoptotic functions under Photofrin-PDT treatment, we knocked down Bax expression using the short hairpin-activated gene silencing system. To generate ASTC-a-1 cell lines that stably suppress the endogenous gene of Bax, we transferred plasmids containing Bax shRNA into cells with G418 as a selective marker. Selection of the transfected cells with nearly complete depletion of Bax required ~1 week of growth in the presence of G418 (Fig. 3A). Both normal cells and Bax RNAi cells were pre-labeled with H_2DCFDA to monitor ROS generation, Rh123 to indicate $\triangle\Psi_m$, calcein along with Co^{2+} to monitor MPT, or Cyt-c-GFP to localize cytochrome *c*. We found that Bax knockdown did not affect Photofrin-PDT-induced mitochondrial apoptotic events including ROS generation (Fig. 3B,C), mitochondrial depolarization (Fig. 4A,B), the long lasting open of MPT pores (Fig. 5A,B) and cytochrome *c* release (Fig. 6A,B). Released cytochrome *c* was also detected in Bax-deficient DU145 cells using immunofluorescence (Fig. 6C) and Western Blotting (Fig. 6D) under Photofrin-PDT treatment. This indicates that Bax is not essential for MOMP caused by Photofrin-PDT.

Bax promotes PDT-induced cell apoptosis through promoting the activation of Drp1

To determine the role of Bax on Photofrin-PDT-induced apoptosis, we compared the apoptosis rate using FCM based on annexin V-FITC/PI double staining in normal ASTC-a-1 cells and Bax RNAi cells after the PDT treatment. We found that Photofrin-PDT resulted in ~90% apoptosis rate in normal cells and ~55% in Bax RNAi cells 6 h post the treatment, indicating that Bax activation plays an important role in the apoptosis (Fig. 7A,B). However, nearly ~90% Bax RNAi cells underwent apoptosis 8 h post-Photofrin-PDT treatment (Fig. 7B), indicating that Bax knockdown fails to prevent the cell death, although it attenuates the susceptibility of cells to PDT.

Next, we explored the modulation of Bax on Drp1 activity during apoptosis induced by Photofrin-PDT. Endogenous Drp1 in normal ASTC-a-1 cells and Bax RNAi cells were detected using immunofluorescence after the PDT treatment. Cells without any treatment were set as control. As shown in Figure 8A, PDT treatment significantly increased the accumulation of Drp1 on mitochondria, indicating that Drp1 is activated by PDT. In contrast, Bax knockdown totally inhibited the stable association of Drp1 with mitochondria, suggesting that Bax is required for Drp1 activation following PDT. Western blotting analysis showed similar result with the confocal data (Fig. 8B).

Furthermore, FCM based on annexin V-FITC/PI double staining was employed to analyze the cell apoptosis rate after Photofrin-PDT treatment in absence of Drp1. We found that Drp1 knockdown resulted in ~70% apoptosis rate after the PDT treatment (Fig. 7A,B), suggesting that Drp1 contributes to Photofrin PDT-induced apoptosis. However, nearly ~90% Drp1 RNAi cells underwent apoptosis 8 h post-PDT treatment (Fig. 7B), similar with the results obtained from Drp1 positive cells (Fig. 7B), indicating that Drp1 knockdown also fails to prevent the cell death finally. We conclude that Bax promotes Photofrin-PDT-induced cell apoptosis through promoting the activation of Drp1. Besides, Bax-mediated mitochondrial translocation of Drp1 is not essential for the apoptosis induced by Photofrin-PDT.

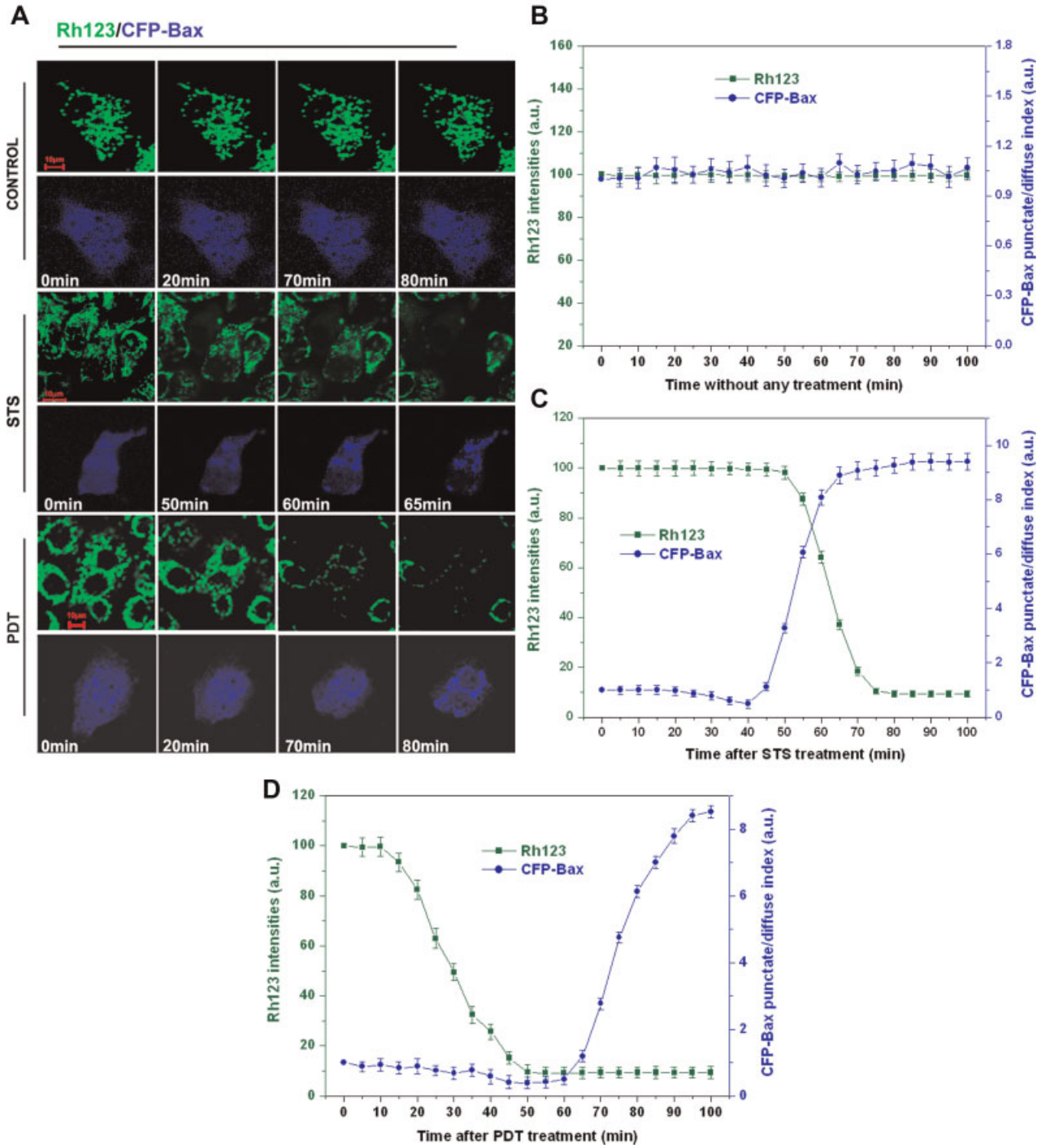

Fig. 1. Bax is activated after mitochondrial depolarization following PDT. A: Representative sequential fluorescent images of ASTC-a-1 cells doubly labeled with Rh123 (green emission) and CFP-Bax (blue emission) to indicate $\Delta\Psi_m$ and Bax localization, respectively, under various treatments. Bar, 10 μm. Quantitative analysis of Rh123 fluorescence emission intensities and CFP-Bax punctate/diffuse index from ASTC-a-1 cells without any treatment (B), treated with STS (C), or treated with Photofrin-PDT (D). Data represent the mean ± SEM (n = 20). STS induced Bax activation (indicated by the mitochondrial translocation of Bax) simultaneously with $\Delta\Psi_m$ dissipation (indicated by the decrease of Rh123 fluorescence), while Photofrin-PDT induced Bax activation after mitochondrial depolarization (indicated by the disappearance of Rh123 fluorescence). PDT, photodynamic therapy; STS, staurosporine; Rh123, rhodamine 123.

In addition, mitochondrial morphology was monitored in normal cells and Drp1 RNAi cells labeled with a mitochondria-target fluorescent probe MitoTracker Deeper Red 633. The mitochondrial network in Drp1 RNAi cells was distinctively longer and more fused than in normal cells (Fig. 8D). We also detected the effect of Drp1 on the release of cytochrome *c* under Photofrin-PDT treatment. To generate ASTC-a-1 cell lines that stably suppressed the endogenous gene of Drp1, we

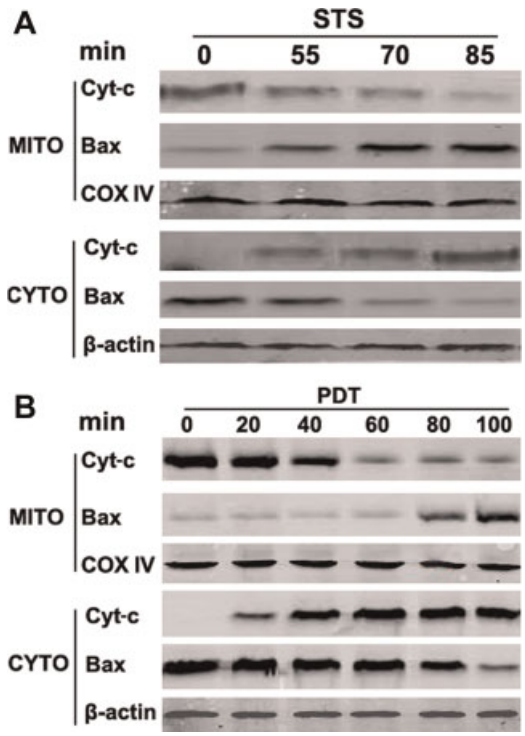

Fig. 2. Bax is activated after the completion of cytochrome *c* release following PDT. ASTC-a-1 cells were treated with STS (A) or Photofrin-PDT (B) and fractionated into cytosol and mitochondria, and analyzed for the distribution of Bax and cytochrome *c* by Western blotting. Fractionation quality was verified by the distribution of specific subcellular markers: COX IV for mitochondria and β-actin for cytosol. The figure is representative of at least three independent experiments. Bax was activated accompanied with cytochrome *c* release caused by STS, while Bax was activated after the completion of cytochrome *c* release by Photofrin-PDT. PDT, photodynamic therapy; STS, staurosporine; Cyt-c, cytochrome *c*; MITO, mitochondria; CYTO, cytosol.

transfected plasmids containing Drp1 shRNA into cells with G418 as a selective marker. Selection of transfected cells with nearly complete depletion of Drp1 required ~1 week of growth in the presence of G418 (Fig. 8C). Both normal cells and Drp1 RNAi cells were transiently transfected with pCyt-c-GFP, and after 48-h expression, cells expressing Cyt-c-GFP were treated with Photofrin-PDT. We found that Drp1 knockdown had no effect on cytochrome *c* release under Photofrin-PDT treatment (Fig. 6A,B), indicating that cytochrome *c* release is not the downstream pro-apoptotic target of Drp1 under the PDT treatment. These results suggest other potential associations between Drp1-mediated mitochondrial fission and cell apoptosis.

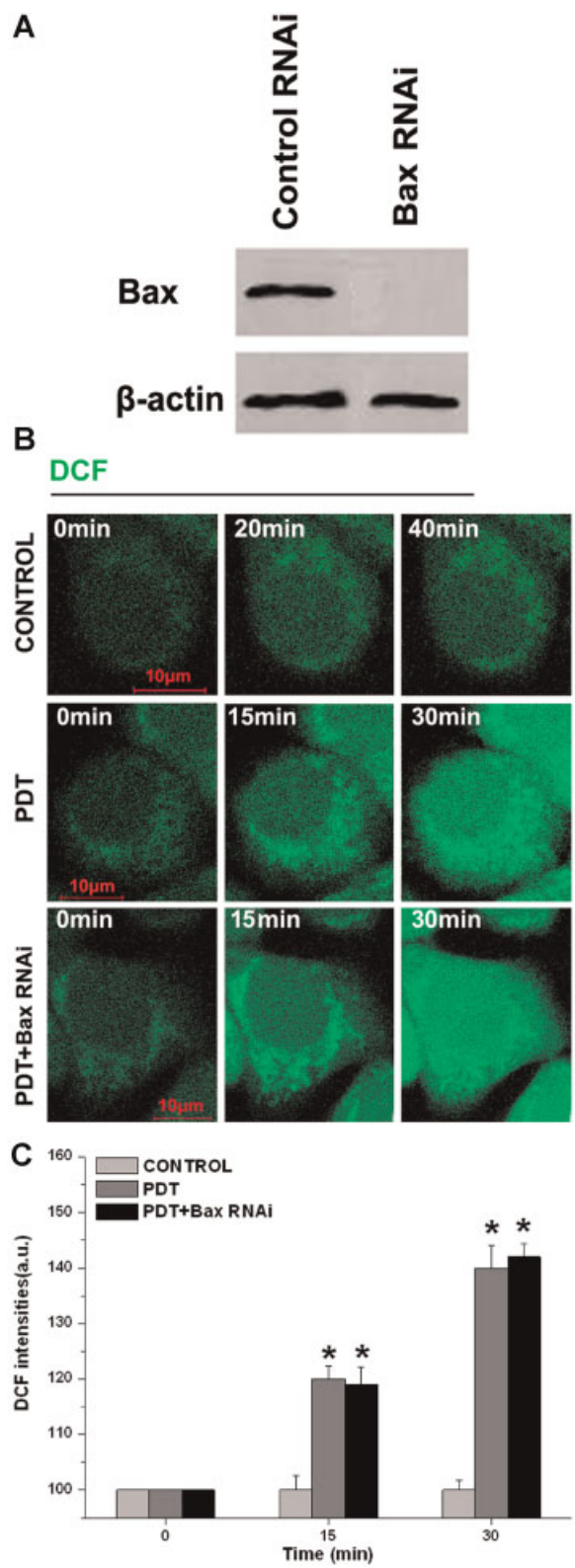

Fig. 3. Knockdown of Bax expression by gene silencing does not affect ROS generation following PDT. A: ASTC-a-1 cells were transfected with plasmids containing shRNA of the target sequence of control or Bax, and the transfectants were selected by growth in media containing G418. Total cell lysates from the control RNAi cells and Bax RNAi cells were prepared, and the expression levels of Bax were analyzed by Western blotting. β-actin level was also analyzed for a loading control. B: Both normal ASTC-a-1 cells and Bax RNAi cells were labeled with DCF (green emission) to monitor ROS generation following Photofrin-PDT. Cells without any treatment were set as control. The figure is representative sequential fluorescent image of at least three independent experiments. Bar, 10 μm. C: Quantitative analysis of DCF fluorescence emission intensities from normal ASTC-a-1 cells or Bax RNAi cells after Photofrin-PDT treatment. Cells without any treatment were set as control. Data represent the mean ± SEM of at least three independent experiments (*$P < 0.05$ vs. control cells). Bax knockdown had no effect on ROS generation following Photofrin-PDT. PDT, photodynamic therapy; DCF, 2′,7′-dichlorofluorescin; RNAi, RNA interference.

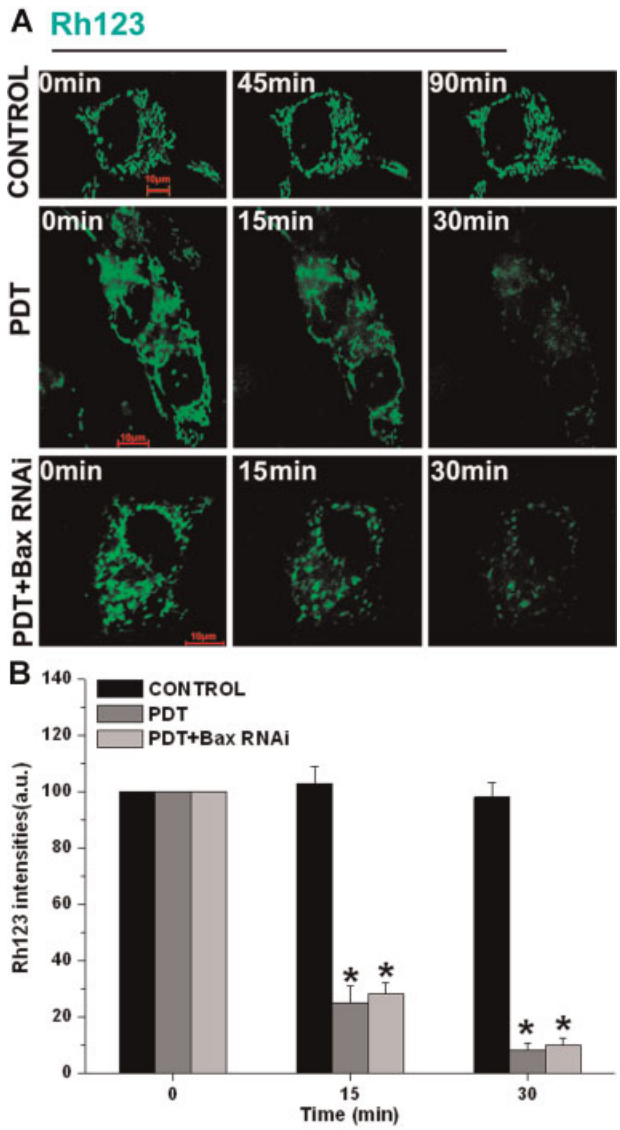

Fig. 4. Knockdown of Bax expression by gene silencing does not affect mitochondrial depolarization following PDT. A: Both normal ASTC-a-1 cells and Bax RNAi cells were labeled with Rh123 (green emission) to indicate $\Delta\Psi_m$ following Photofrin-PDT. Cells without any treatment were set as control. The figure is representative sequential fluorescent image of at least three independent experiments. Bar, 10 μm. B: Quantitative analysis of Rh123 fluorescence emission intensities from normal ASTC-a-1 cells or Bax RNAi cells after Photofrin-PDT treatment. Cells without any treatment were set as control. Data represent the mean ± SEM of at least three independent experiments (*$P < 0.05$ vs. control cells). Bax knockdown had no effect on mitochondrial depolarization following Photofrin-PDT. PDT, photodynamic therapy; Rh123, rhodamine 123; RNAi. RNA interference.

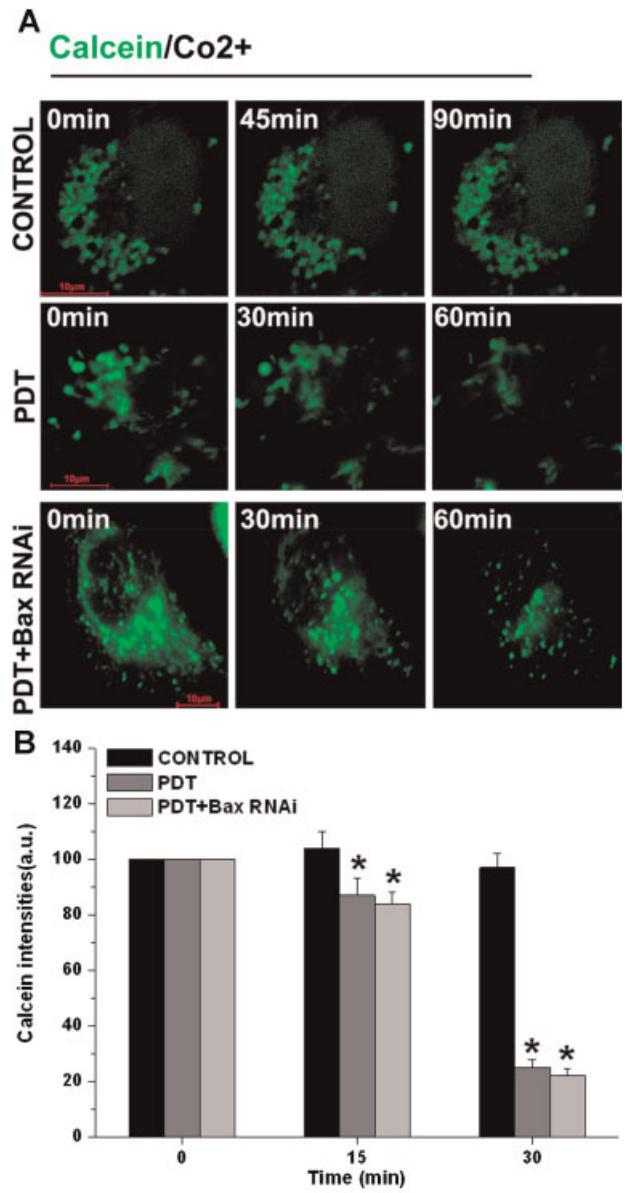

Fig. 5. Knockdown of Bax expression by gene silencing does not affect the long lasting open of MPT pores following PDT. A: Both normal ASTC-a-1 cells and Bax RNAi cells were labeled with calcein/Co^{2+} (green emission) to indicate the state of opening of MPT pores following Photofrin-PDT. Cells without any treatment were set as control. The figure is representative sequential fluorescent image of at least three independent experiments. Bar, 10 μm. B: Quantitative analysis of calcein fluorescence emission intensities from normal ASTC-a-1 cells or Bax RNAi cells after PDT treatment. Cells without any treatment were set as control. Data represent the mean ± SEM of at least three independent experiments (*$P < 0.05$ vs. control cells). Bax knockdown had no effect on the long lasting open of MPT pores following Photofrin-PDT. PDT, photodynamic therapy; RNAi, RNA interference.

Signaling pathways involved in Bax activation upon PDT treatment

To obtain better mechanistic insight of Bax activation in ASTC-a-1 cells treated with Photofrin-PDT, we tested activities of protein kinase Cδ (PKCδ) (labeled by GFP-PKCδ), Bim L (labeled by GFP-Bim L), and glycogen synthase kinase 3β (GSK3β) (labeled by YFP-GSK3β) (Fig. 9A), all of which were involved in Bax activation upon various stimuli. GFP-PKCδ and GFP-Bim L accumulated on mitochondria and YFP-GSK3β translocated to nucleus in 1 h post-Photofrin-PDT treatment, all the phenomenon indicating activation of the three proteins following PDT. We found that GFP-PKCδ, GFP-Bim L, and YFP-GSK3β were all activated at the time before Bax activation (Fig. 1D), suggesting that Bax activation by Photofrin-PDT may be modulated by PKCδ, Bim L, and/or GSK3β.

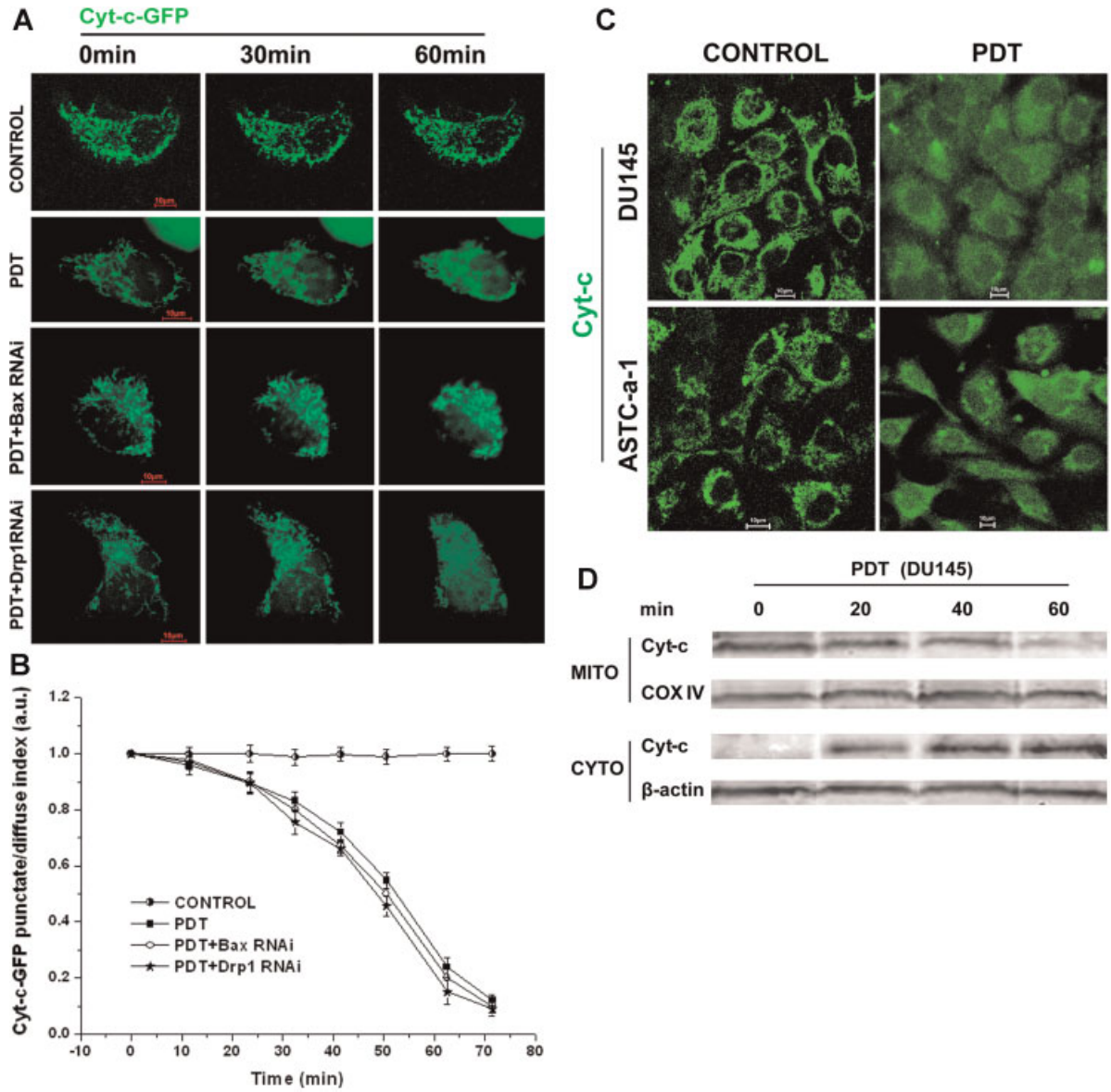

Fig. 6. Neither Bax nor Drp1 is required for cytochrome *c* release following PDT. A: Normal ASTC-a-1 cells, Bax RNAi cells or Drp1 RNAi cells transiently expressing Cyt-c-GFP (green emission) were treated with Photofrin-PDT. Cells without any treatment were set as control. The figure is representative sequential fluorescent image of at least three independent experiments. Bar, 10 μm. B: Quantitative analysis of Cyt-c-GFP punctuate/diffuse index in normal ASTC-a-1 cells, Bax RNAi cells or Drp1 RNAi cells following Photofrin-PDT. Cells without any treatment were set as control. Data represent the mean ± SEM (n = 20). Neither Bax nor Drp1 knockdown had effect on cytochrome *c* release following Photofrin-PDT. C: Endogenous cytochrome *c* in ASTC-a-1 cells and DU145 cells was detected using immunofluorescence with anti-cytochrome *c* antibody (green emission) under Photofrin-PDT treatment. Cells without any treatment were set as control. The figure is representative fluorescent image of at least three independent experiments. Bar, 10 μm. D: DU145 cells were treated with Photofrin-PDT and fractionated into cytosol and mitochondria, and analyzed for the distribution of cytochrome *c* by Western blotting. Fractionation quality was verified by the distribution of specific subcellular markers: COX IV for mitochondria and β-actin for cytosol. The figure shown is representative of at least three independent experiments. Photofrin-PDT resulted in cytochrome *c* release in both ASTC-a-1 cells and DU145 cells. PDT, photodynamic therapy; Cyt-c, cytochrome *c*; RNAi, RNA interference; ASTC-a-1, human lung adenocarcinoma cells; DU145, human prostate carcinoma cells; MITO, mitochondria; CYTO, cytosol.

Levels of cell death by Photofrin-PDT in cells under various pre-treatments were analyzed using FCM based on annexin V-FITC/PI double staining (Fig. 9B). We found that PKCδ inhibition by GÖ6983 resulted in nearly the same level of apoptosis reduction as Bax knockdown. Bim knockdown caused higher level of apoptosis reduction than GSK-3β inhibition by LiCl. Ascorbic acid exposure resulted in the highest level of apoptosis reduction of all. These results demonstrate that all the three proteins of PKCδ, Bim L, and GSK-3β are involved in apoptosis induced by Photofrin-PDT probably through promoting Bax activation.

Discussion

In the present study, we report that Bax activation is not essential for MOMP but essential for Drp1-mediated

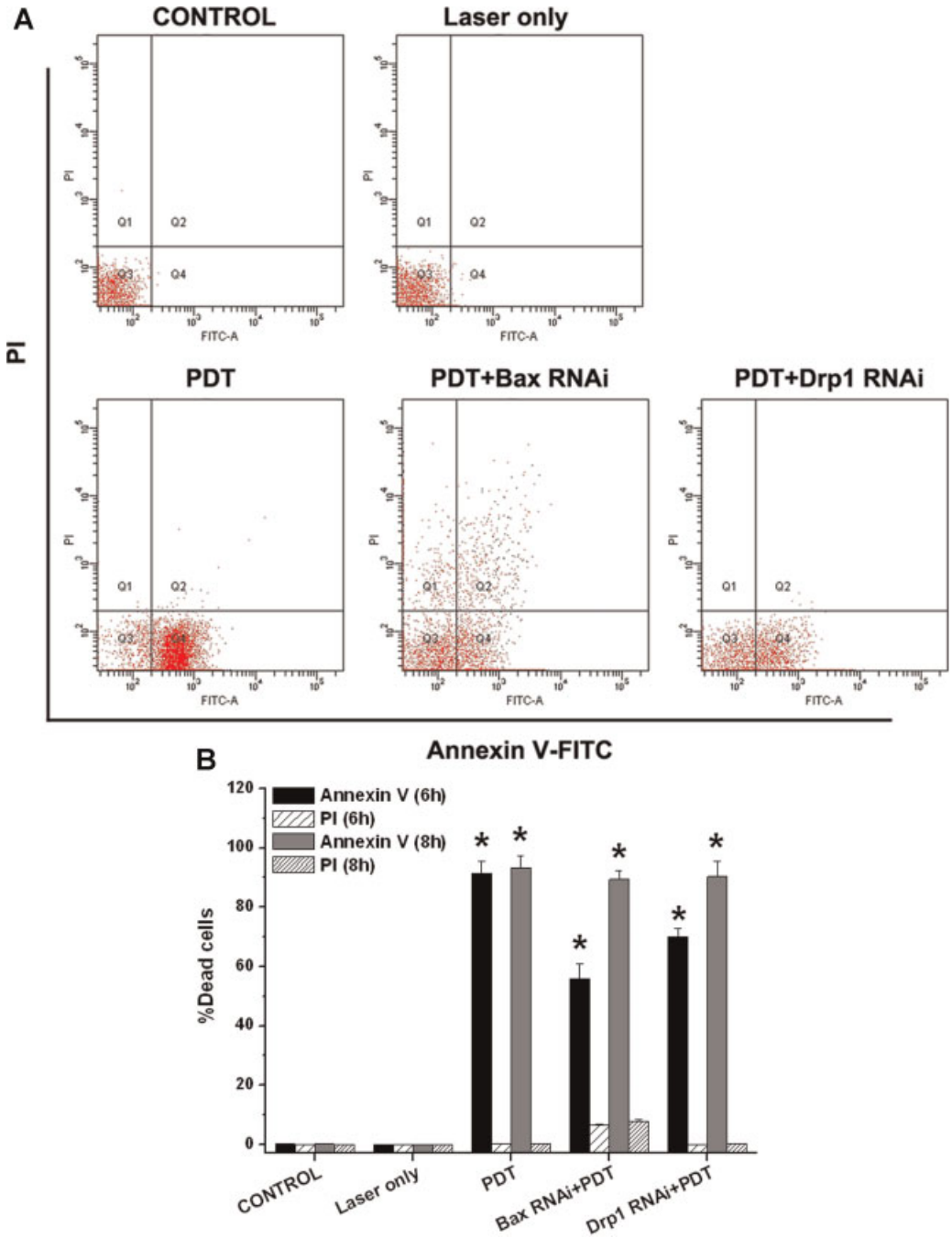

Fig. 7. Knockdown of Bax and Drp1 expression by gene silencing both inhibit PDT-induced apoptosis. A: Representative dot plots for ASTC-a-1 cell death analysis after various treatments using FCM based on annexin V-FITC/PI double staining. B: The percentage of ASTC-a-1 cells positively stained with annexin V-FITC or PI dyes after various treatments was analyzed by FCM. Data represent the mean ± SEM of at least three independent experiments (*$P < 0.05$ vs. control cells). Both Bax and Drp1 knockdown inhibited cell apoptosis, but not changed the cell death fate following Photofrin-PDT. PDT, photodynamic therapy; RNAi, RNA interference; Drp1, dynamin-related protein.

mitochondrial fission caused by Photofrin-PDT. Besides, PKCδ, Bim L and GSK3β are all activated and probably involved in Bax activation and thus promote Photofrin-PDT-induced apoptosis.

Apoptosis-associated MOMP is known to require Bax and/or Bak, two closely related members of the Bcl-2 family (Wolter et al., 1997; Wei et al., 2001; Youle and Strasser, 2008). In STS-treated cells (Rüegg and Burgess, 1989; Chae et al., 2000; Karaman et al., 2008), Bax was activated simultaneously with mitochondrial depolarization and cytochrome *c* release, indicating a crucial role of Bax on MOMP (Figs. 1 and 2). However, under Photofrin-PDT treatment, Bax was activated after MOMP and Bax knockdown did not affect MOMP, suggesting that Bax activation is not required for MOMP (Figs. 1–6). It is probably because that Photofrin-PDT-induced apoptosis is initiated from directly mitochondrial photodamage (Wu et al., 2006a,b), differed from the apoptosis caused by some other stimuli, such as STS and DNA injury. Upon these stimuli, pro-apoptotic BH3 proteins are activated and interact

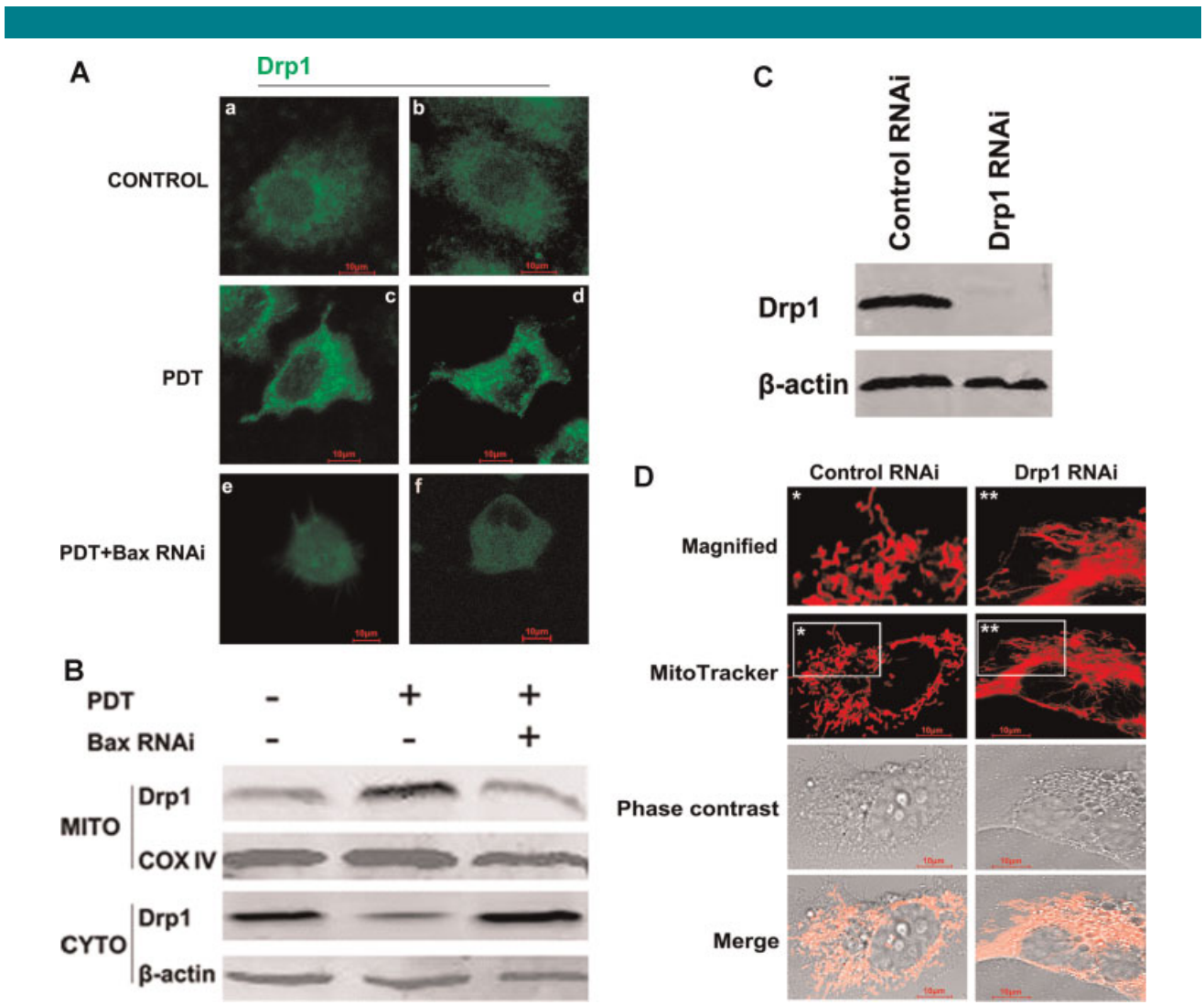

Fig. 8. Knockdown of Bax expression by gene silencing totally inhibits the activation of mitochondrial fission protein Drp1 following PDT. A: Endogenous Drp1 in normal ASTC-a-1 cells (c,d) and Bax RNAi cells (e,f) were detected by immunofluorescence with anti-Drp1 antibody (green emission) after Photofrin-PDT. Cells without any treatment were set as control (a,b). The figure is representative fluorescent image of at least three independent experiments. Bar, 10 μm. B: Both normal ASTC-a-1 cells and Bax RNAi cells were treated with Photofrin-PDT and fractionated into cytosol and mitochondria, and analyzed for the distribution of Drp1 by Western blotting. Fractionation quality was verified by the distribution of specific subcellular markers: COX IV for mitochondria and β-actin for cytosol. The figure is representative of at least three independent experiments. Bax knockdown resulted in total inhibition of Drp1 activation (indicated by the increased mitochondrial accumulation of Drp1) following Photofrin-PDT, suggesting that Bax is required for Drp1 activation under the PDT treatment. C: ASTC-a-1 cells were transfected with plasmids containing shRNA of the target sequence of control or Drp1, and the transfectants were selected by growth in media containing G418. Total cell lysates from the control RNAi cells and Drp1 RNAi cells were prepared, and the expression levels of Drp1 were analyzed by Western blotting. β-Actin level was also analyzed for a loading control. D: Mitochondria of control ASTC-a-1 RNAi cells or Drp1 RNAi cells were visualized with MitoTracker Deeper Red 633 and analyzed by confocal microscopy. Enlargements are shown for detailed structure of mitochondria. Bar, 10 μm. Drp1 knockdown caused elongated mitochondria. PDT, photodynamic therapy; RNAi, RNA interference; Drp1, dynamin-related protein; MITO, mitochondria; CYTO, cytosol.

with and inhibit anti-apoptotic Bcl2 or Bcl-X_L. Thus, Bax and Bak are free to induce mitochondrial permeabilization with release of cytochrome *c* (Hotchkiss et al., 2009). It is known that the intracellular localization of the photosensitizer coincides with the primary site of photodamage, mainly due to the limited diffusion of the short-lived singlet oxygen, which is thought to be the predominant oxidant in PDT (Dougherty et al., 1998; Dougherty, 2002; Oleinick et al., 2002). Hence the local photodamage to specific subcellular targets critically influences the kinetics and the regulatory pathways activated by PDT. Release of cytochrome *c* is shown to occur immediately after PDT with photosensitizer verteporfin, of which mitochondrial adenine nucleotide translocator (ANT) is reported to be a critical target (Granville et al., 1998; Belzacq et al., 2001). Kessel and Luo (1999) demonstrate that cytochrome *c* is released simultaneously with the loss of $\Delta\Psi_m$, both events occurring immediately after PDT with photosensitizer porphycenes. Similarly, PDT with hypericin or hypocrellin, also mitochondrion-localized photosensitizers, induces rapid collapse of $\Delta\Psi_m$ (Chaloupka et al., 1999). Results obtained in the present study show that with increased mitochondrial ROS generation (Fig. 3B,C), cytochrome *c* release (Fig. 6A,B) and $\Delta\Psi_m$ dissipation (Fig. 1A,D) immediately occurs after Photofrin-PDT treatment. These results reveal that photoactivation of mitochondria-targeted photosensitizers can directly cause MOMP following PDT. However, we cannot rule

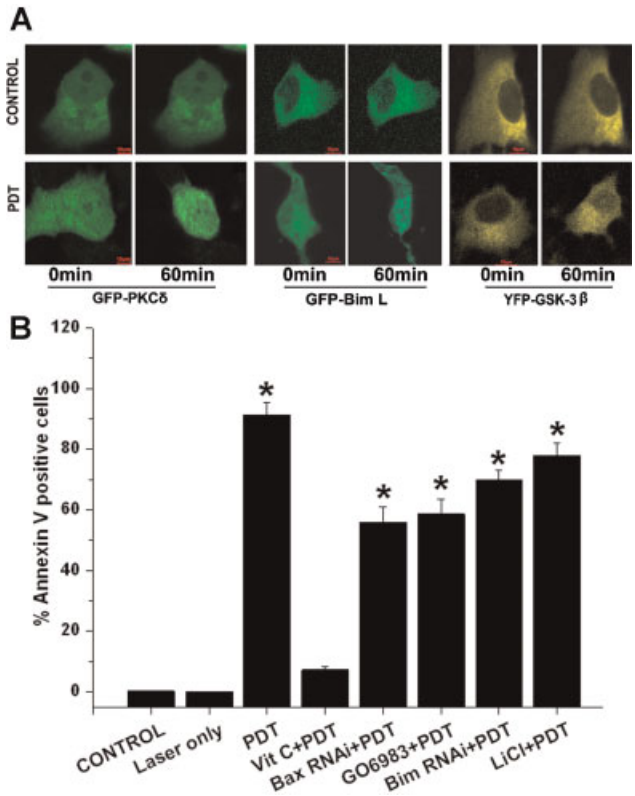

Fig. 9. PKCδ, Bim L, and GSK3β are activated and may be involved in Bax activation following PDT. A: ASTC-a-1 cells transiently expressing GFP-PKCδ (green emission), GFP-Bim L (green emission) or YFP-GSK3β (yellow emission) were treated with Photofrin-PDT. Cells without any treatment were set as control. The figure shown is representative fluorescent image of at least three independent experiments. Bar, 10 μm. B: Quantitative analysis of cell death by FCM based on annexin V-FITC/PI double staining was performed in ASTC-a-1 cells treated with Photofrin-PDT in the presence of GÖ6983, LiCl, ascorbic acid, or in the absence of Bim. Data represent the mean ± SEM of at least three independent experiments (*$P < 0.05$ vs. control cells). PKCδ, Bim L, and GSK3β were activated and may be involved in Bax activation following Photofrin-PDT. PDT, photodynamic therapy; RNAi, RNA interference; Vit C, ascorbic acid; PKCδ, protein kinase Cδ; GSK3β, glycogen synthase kinase 3β.

out the contribution of Bak on MOMP in Bax RNAi cells, since Bak often plays a redundant role of Bax and can induce cytochrome *c* release in the absence of Bax (Wei et al., 2001; Degenhardt et al., 2002; Youle and Strasser, 2008).

Bax can be activated on the modulation of several cytosolic signaling pathways under oxidative stress. For example, GSK-3β can be activated by ROS (King and Jope, 2005) and thus promotes Bax activation through direct phosphorylation of Bax (Linseman et al., 2004) or through reduction of Mcl-1 cellular protein levels (Maurer et al., 2006). In addition, ROS/ASK1/JNK/Bim L/Bax pathway has also been reported to participate in Bax activation under the conditions of intracellular oxidative stress (Gotoh and Cooper, 1998; Tobiume et al., 2001; Lei and Davis, 2003; Laethem et al., 2006). Besides, Majumder et al. (2001) have reported the targeting of PKCδ to mitochondria in oxidative stress response. PKCδ can degrade Mcl-1 to trigger apoptosis by promoting Bax activation (Sitailo et al., 2006). However, how Bax was activated by PDT-induced oxidative stress is still not well understood. In the present study, PKCδ, Bim L, and GSK-3β were all activated by Photofrin-PDT, and thus could contribute to Bax activation under the treatment.

The importance of mitochondria as targets for the initiation of apoptosis by PDT has been convincingly demonstrated by Kessel et al. (1997) and Kessel and Luo (1998, 1999). These investigators tested a series of photosensitizers for their preferential localization as well as their ability to photosensitize cells to apoptosis. They found that those photosensitizers that bound to mitochondria induced apoptosis upon photoirradiation, whereas those that bound to the plasma membrane or lysosomes, but not mitochondria, killed cells less efficiently. We believe that the selectivity for mitochondrial target of photosensitizer is crucial for the mode of MOMP following PDT. The phthalocyanine (Pc 4) photosensitizer preferentially binds to the endoplasmic reticulum, Golgi complex, and mitochondria and induces rapid apoptotic cell death after exposure to light (Agarwal et al., 1993; Trivedi et al., 2000). The relatively poor mitochondrial selectivity of Pc 4 in comparison with the high selectivity of Photofrin may cause MOMP through mechanisms other than direct photodamage on mitochondria. The proposal has been confirmed by Oleinick et al. showing that Bax is essential for cytochrome *c* release but not for cell death caused by Pc 4-PDT (Chiu et al., 2003). They also report that Pc 4-PDT-induced release of the mitochondrial pro-apoptotic proteins cytochrome *c* and Smac/DIABLO depends on Bax and is blocked in Bax-deficient DU145 cells (Usuda et al., 2002).

Although Bax activation was not essential for MOMP induced by Photofrin-PDT, we found that Bax knockdown did attenuate the susceptibility of cells to PDT (Fig. 7). The fact gave us an idea to find new pro-apoptotic targets of Bax. Mitochondrial fission often occurs during apoptosis. It is reported that activation of Bax and/or Bak leads rapidly to mitochondrial fragmentation (Frank et al., 2001; Kowaltowski et al., 2002; Karbowski et al., 2004). Mitochondrial fission is also regulated by a GTPase Drp1, which can form ring-like oligomers at specific points along mitochondria (Smirnova et al., 2001; Yoon et al., 2001). Bax/Bak promotes sumoylation of Drp1 and its stable association with mitochondria during apoptosis (Wasiak et al., 2007). We found that Bax has tight correlation with Drp1, because silencing of Bax completely ceased the stable association of Drp1 with mitochondria following PDT (Fig. 8A,B). We also found that knockdown of Drp1 inhibited Photofrin-PDT-induced apoptosis (Fig. 7) without any effect on cytochrome *c* release (Fig. 6A,B). A dominant-negative mutant of Drp1 (Drp1K38A) that can impair mitochondrial fission has been observed to impair cytochrome *c* release and delay cell death in response to some pro-apoptotic agents (Frank et al., 2001; Brooks et al., 2007). However, it should be noted that the delay in cytochrome *c* release observed is relatively modest and has not been shown to translate into long-term survival. The delayed kinetics of cytochrome *c* release seen when Drp1 expression is ablated or functionally impaired may be a non-physiological byproduct of altered mitochondrial ultrastructure in such cells, because the release kinetics of Smac, Omi, adenylate kinase 2, and other intermembrane space proteins was unaltered under the same conditions (Parone et al., 2006; Estaquier and Arnoult, 2007; Ishihara et al., 2009). One possible reason for this is that remodeling of the cristae junctions in such cells—known to be required for efficient cytochrome *c* release (Scorrano et al., 2002)—may be affected. However, because the release kinetics of Smac, Omi, adenylate kinase 2, and other intermembrane space proteins is overtly normal, this suggests that MOMP is unaffected through loss of Drp1. Our results show that silencing of Drp1 has no effect on cytochrome *c* release may be an evidence of the view. Other than this view, our result can also be interpreted that Drp1 has no effect spatio-temporally on MOMP following Photofrin-PDT, since mitochondrial association of Drp1 occurred after MOMP. Great effort should be made to uncover the mechanism of Drp1-mediated cell apoptosis. Aside from influencing

mitochondrial morphology and degree of connectivity of mitochondrial networks, mitochondrial fission/fusion contributes to reparation of defective mitochondria, proper segregation of mitochondria into daughter cells during cell division, the efficiency of oxidative phosphorylation and intramitochondrial calcium signal propagation (Chan, 2006). We believe that Drp1-mediated fragmentation, a morphological change of mitochondria, increases the susceptibility of cells to apoptotic stimuli with some unknown mechanisms and the fragmentation might be a positive feedback regulation of apoptosis. Actually, we found that Drp1 knockdown only slightly inhibited PDT-induced cell apoptosis (~20%) (Fig. 7A,B), and these data may suggest that Drp1 is not a main mediator for PDT-induced cell apoptosis. Besides, it is likely that although Bax knockdown attenuates the susceptibility of cells to PDT (Fig. 7A,B), it does not change the cell death fate (Fig. 7B), since cytochrome *c* release to cytoplasm is sufficient to induce apoptosis in the absence of Bax (Youle and Strasser, 2008; Hotchkiss et al., 2009).

PDT is the most important adjuvant treatment modality for tumor except for radiotherapy and chemotherapy. Understanding the mechanisms involved in PDT-mediated apoptosis may improve its therapeutic efficacy. Here, we reported that Bax activation was not essential for MOMP but essential for Drp1-mediated mitochondrial fission during apoptosis caused by Photofrin-PDT. It is the first time to report that fission-associated proteins were involved in PDT-induced apoptosis.

Acknowledgments

We thank Prof. Jonh H. Kehrl (Laboratory of Immunoregulation, National Institute of Allergy and Infectious Diseases, National Institutes of Health) for kindly providing pEYFP-GSK3β; Prof. Yukiko Gotoh (the Institute of Molecular and Cellular Bioscience, University of Tokyo) and Prof. Gilmore (The School of Biological Sciences, University of Manchester) for kindly providing pDsRed-mit and pCFP-Bax, respectively; Prof. Richard J. Youle (National Institutes of Health) for kindly providing pYFP-Drp1; Prof. Jean-Claude Martinou (University of Geneva) for kindly providing pshRNA Drp1; Prof. Gregory J. Gores (Mayo Medical School, Clinic, and Foundation) for kindly providing p Cyt-c-GFP; Prof. Yusuf A. Hannun (Department of Biochemistry and Molecular Biology, Medical University of South Carolina) for kindly providing GFP-PKCδ. This research is supported by the National Basic Research Program of China (2010CB732602), the Program for Changjiang Scholars and Innovative Research Team in University (IRT0829), and the National Natural Science Foundation of China (30870676 and 30870658). The funders had no role in study design, data collection and analysis, decision to publish, or preparation of the manuscript.

Literature Cited

Agarwal ML, Larkin HE, Zaidi SI, Mukhtar H, Oleinick NL. 1993. Phospholipase activation triggers apoptosis in photosensitized mouse lymphoma cells. Cancer Res 53:5897–5902.
Agostinis P, Buytaert E, Breyssens H, Hendrickx N. 2004. Regulatory pathways in photodynamic therapy induced apoptosis. Photochem Photobiol Sci 3:721–729.
Arnoult D, Grodet A, Lee YJ, Estaquier J, Blackstone C. 2005. Release of OPA1 during apoptosis participates in the rapid and complete release of cytochrome *c* and subsequent mitochondrial fragmentation. J Biol Chem 280:35742–35750.
Belzacq AS, Jacotot E, Vieira HL, Mistro D, Granville DJ, Xie Z, Reed JC, Kroemer G, Brenner C. 2001. Apoptosis induction by the photosensitizer Verteporfin: Identification of mitochondrial adenine nucleotide translocator as a critical target. Cancer Res 61:1260–1264.
Brooks C, Wei Q, Feng L, Dong G, Tao Y, Mei L, Xie ZJ, Dong Z. 2007. Bak regulates mitochondrial morphology and pathology during apoptosis by interacting with mitofusins. Proc Natl Acad Sci USA 104:11649–11654.
Carthy CM, Granville DJ, Jiang H, Levy JG, Rudin CM, Thompson CB, McManus BM, Hunt DW. 1999. Early release of mitochondrial cytochrome *c* and expression of mitochondrial epitope 7A6 with aporphyrin-derived photosensitizer: Bcl-2 and Bcl-xL overexpression do not prevent early mitochondrial events but still depress caspase activity. Lab Invest 79:953–965.
Chae HJ, Kang JS, Byun JO, Han KS, Kim DU, Oh SM, Kim HM, Chae SW, Kim HR. 2000. Molecular mechanism of staurosporine-induced apoptosis in osteoblasts. Pharmacol Res 42:373–381.
Chaloupka R, Obsil T, Plásek J, Sureau F. 1999. The effect of hypericin and hypocrellin—A on lipid membranes and membrane potential of 3T3 fibroblasts. Biochim Biophys Acta 1418:39–47.
Chan DC. 2006. Mitochondria: Dynamic organelles in disease, aging, and development. Cell 125:1241–1252.
Chen M, Xing D, Chen T, Zhang L. 2007. Bim L involvement in Bax activation during UV irradiation-induced apoptosis. Biochem Biophys Res Commun 358:559–565.
Chipuk JE, Moldoveanu T, Llambi F, Parsons MJ, Green DR. 2010. The Bcl-2 family reunion. Mol Cell 37:299–310.
Chiu SM, Oleinick NL. 2001. Dissociation of mitochondrial depolarization from cytochrome *c* release during apoptosis induced by photodynamic therapy. Br J Cancer 84:1099–1106.
Chiu SM, Evans HH, Lam M, Nieminen AL, Oleinick NL. 2001. Phthalocyanine 4 photodynamic therapy-induced apoptosis of mouse L5178Y-R cells results from a delayed but extensive release of cytochrome c from mitochondria. Cancer Lett 165:51–58.
Chiu SM, Xue LY, Usuda J, Azizuddin K, Oleinick NL. 2003. Bax is essential for mitochondrion-mediated apoptosis but not for cell death caused by photodynamic therapy. Br J Cancer 89:1590–1597.
Degenhardt K, Sundararajan R, Lindsten T, Thompson C, White E. 2002. Bax and Bak independently promote cytochrome c release from mitochondria. J Biol Chem 277:14127–14134.
Delivani P, Adrain C, Taylor RC, Duriez PJ, Martin SJ. 2006. Role for CED-9 and Egl-1 as regulators of mitochondrial fission and fusion dynamics. Mol Cell 21:761–773.
Desagher S, Martinou JC. 2000. Mitochondria as the central control point of apoptosis. Trends Cell Biol 10:369–377.
Dougherty TG. 2002. An update on photodynamic therapy applications. J Clin Laser Med Surg 20:3–7.
Dougherty TG, Gomer CJ, Henderson BW, Jori G, Kessel D, Korbelik M, Moan J, Peng Q. 1998. Photodynamic therapy. J Natl Cancer Inst 90:889–905.
Estaquier J, Arnoult D. 2007. Inhibiting Drp1-mediated mitochondrial fission selectively prevents the release of cytochrome *c* during apoptosis. Cell Death Differ 14:1086–1094.
Frank S, Gaume B, Bergmann-Leitner ES, Leitner WW, Robert EG, Catez F, Smith CL, Youle RJ. 2001. The role of dynamin-related protein 1, a mediator of mitochondrial fission, in apoptosis. Dev Cell 1:515–525.
Gotoh Y, Cooper JA. 1998. Reactive oxygen species- and dimerization-induced activation of apoptosis signal-regulating kinase 1 in tumor necrosis factor-alpha signal transduction. J Biol Chem 273:17477–17482.
Granville DJ, Carthy CM, Jiang H, Shore GC, McManus BM, Hunt DWC. 1998. Rapid cytochrome c release, activation of caspases 3, 6, 7 and 8 followed by Bap31 cleavage in HeLa cells treated with photodynamic therapy. FEBS Lett 437:5–10.
Granville DJ, Shaw JR, Leong S, Carthy CM, Margaron P, Hunt DW, McManus BM. 1999. Release of cytochrome c, Bax migration, Bid cleavage, and activation of caspases 2, 3, 6, 7, 8, and 9 during endothelial cell apoptosis. Am J Pathol 155:1021–1025.
He J, Whitacre CM, Xue LY, Berger NA, Oleinick NL. 1998. Protease activation and cleavage of poly (ADP-ribose) polymerase: An integral part of apoptosis in response to photodynamic treatment. Cancer Res 58:940–946.
Hotchkiss RS, Strasser A, McDunn JE, Swanson PE. 2009. Cell death. N Engl J Med 361:1570–1583.
Ishihara N, Nomura M, Jofuku A, Kato H, Suzuki SO, Masuda K, Otera H, Nakanishi Y, Nonaka I, Goto Y, Taguchi N, Morinaga H, Maeda M, Takayanagi R, Yokota S, Mihara K. 2009. Mitochondrial fission factor Drp1 is essential for embryonic development and synapse formation in mice. Nat Cell Biol 11:958–966.
Karaman MW, Herrgard S, Treiber DK, Gallant P, Atteridge CE, Campbell BT, Chan KW, Ciceri P, Davis MI, Edeen PT, Faraoni R, Floyd M, Hunt JP, Lockhart DJ, Milanov ZV, Morrison MJ, Pallares G, Patel HK, Pritchard S, Wodicka LM, Zarrinkar PP. 2008. A quantitative analysis of kinase inhibitor selectivity. Nat Biotechnol 26:127–132.
Karbowski M, Arnoult D, Chen H, Chan DC, Smith CL, Youle RJ. 2004. Quantitation of mitochondrial dynamics by photolabeling of individual organelles shows that mitochondrial fusion is blocked during the Bax activation phase of apoptosis. J Cell Biol 164:493–499.
Karbowski M, Norris KL, Cleland MM, Jeong SY, Youle RJ. 2006. Role of Bax and Bak in mitochondrial morphogenesis. Nature 443:658–662.
Kessel D, Luo Y. 1998. Mitochondrial photodamage and PDT-induced apoptosis. J Photochem Photobiol B 42:89–95.
Kessel D, Luo Y. 1999. Photodynamic therapy: A mitochondrial inducer of apoptosis. Cell Death Differ 6:28–35.
Kessel D, Luo Y, Deng Y, Chang CK. 1997. The role of subcellular localization in initiation of apoptosis by photodynamic therapy. Photochem Photobiol 65:422–426.
Kim HR, Luo Y, Li G, Kessel D. 1999. Enhanced apoptotic response to photodynamic therapy after bcl-2 transfection. Cancer Res 59:3429–3432.
King TD, Jope RS. 2005. Inhibition of GSK3 protects cells from intrinsic but not extrinsic oxidative stress. Neuroreport 16:597–601.
Kowaltowski AJ, Cosso RG, Campos CB, Fiskum G. 2002. Effect of Bcl-2 overexpression on mitochondrial structure and function. J Biol Chem 277:42802–42807.
Laethem V, Nys AK, Van Kelst S, Claerhout S, Ichijo H, Vandenheede JR, Garmyn M, Agostinis P. 2006. Apoptosis signal regulating kinase-1 connects reactive oxygen species to p38 MAPK-induced mitochondrial apoptosis in UVB-irradiated human keratinocytes. Free Radic Biol Med 41:1361–1371.
Lei K, Davis RJ. 2003. JNK phosphorylation of Bim-related members of the Bcl2 family induces Bax-dependent apoptosis. Proc Natl Acad Sci USA 100:2432–2437.
Linseman DA, Butts BD, Precht TA, Phelps RA, Le SS, Laessig TA, Bouchard RJ, Florez-McClure ML, Heidenreich KA. 2004. Glycogen synthase kinase-3β phosphorylates bax and promotes its mitochondrial localization during neuronal apoptosis. J Neurosci 24:9993–10002.
Majumder PK, Mishra NC, Sun X, Bharti A, Kharbanda S, Saxena S, Kufe D. 2001. Targeting of protein kinase C δ to mitochondria in the oxidative stress response. Cell Growth Differ 12:465–470.
Maurer U, Charvet C, Wagman AS, Dejardin E, Green DR. 2006. Glycogen synthase kinase-3 regulates mitochondrial outer membrane permeabilization. Mol Cell 21:749–760.
Oleinick NL, Morris RL, Belichenko I. 2002. The role of apoptosis in response to photodynamic therapy: What, where, why, and how. Photochem Photobiol Sci 1:1–21.
Parone PA, James DI, Da Cruz S, Mattenberger Y, Donze O, Barja F, Martinou JC. 2006. Inhibiting the mitochondrial fission machinery does not prevent Bax/Bak-dependent apoptosis. Mol Cell Biol 26:7397–7408.
Rousset N, Vonarx V, Eléouet S, Carré J, Bourré L, Lajat Y, Patrice T. 2000. Cellular distribution and phototoxicity of benzoporphyrin derivative and Photofrin. Res Exp Med (Berl) 199:341–357.

Rüegg UT, Burgess GM. 1989. Staurosporine, K-252 and UCN-01: Potent but nonspecific inhibitors of protein kinases. Trends Pharmacol Sci 10:218–220.
Scorrano L, Ashiya M, Buttle K, Weiler S, Oakes SA, Mannella CA, Korsmeyer SJ. 2002. A distinct pathway remodels mitochondrial cristae and mobilizes cytochrome *c* during apoptosis. Dev Cell 2:55–67.
Sheridan C, Delivani P, Cullen SP, Martin SJ. 2008. Bax- or Bak-induced mitochondrial fission can be uncoupled from cytochrome *c* release. Mol Cell 31:570–585.
Sitailo LA, Tibudan SS, Denning MF. 2006. The protein kinase C δ catalytic fragment targets Mcl-1 for degradation to trigger apoptosis. J Biol Chem 281:29703–29710.
Smirnova E, Griparic L, Shurland DL, van der Bliek AM. 2001. Dynamin-related protein Drp1 is required for mitochondrial division in mammalian cells. Mol Biol Cell 2: 2245–2256.
Taylor RC, Cullen SP, Martin SJ. 2008. Apoptosis: Controlled demolition at the cellular level. Nat Rev Mol Cell Biol 9:231–241.
Tobiume K, Matsuzawa A, Takahashi T, Nishitoh H, Morita K, Takeda K, Minowa O, Miyazono K, Noda T, Ichijo H. 2001. ASK1 is required for sustained activations of JNK/p38 MAP kinases and apoptosis. EMBO Rep 2:222–228.
Triesscheijn M, Baas P, Schellens JHM, Stewart FA. 2006. Photodynamic therapy in oncology. Oncologist 11:1034–1044.
Trivedi NS, Wang HW, Nieminen AL, Oleinick NL, Izatt JA. 2000. Quantitative analysis of Pc 4 localization in mouse lymphoma (LY-R) cells via double-label confocal fluorescence microscopy. Photochem Photobiol 71:634–639.
Usuda J, Chiu SM, Azizuddin K, Xue LY, Lam M, Nieminen AL, Oleinick NL. 2002. Promotion of photodynamic therapy-induced apoptosis by the mitochondrial protein Smac/DIABLO: Dependence on Bax. Photochem Photobiol 76:217–223.
Varnes ME, Chiu SM, Xue LY, Oleinick NL. 1999. Photodynamic therapy induced apoptosis in lymphoma cells: Translocation of cytochrome *c* causes inhibition of respiration as well as caspase activation. Biochem Biophys Res Commun 255:673–679.
Wasiak S, Zunino R, McBride HM. 2007. Bax/Bak promote sumoylation of DRP1 and its stable association with mitochondria during apoptotic cell death. J Cell Biol 177:439–450.
Wei MC, Zong WX, Cheng EH, Lindsten T, Panoutsakopoulou V, Ross AJ, Roth KA, MacGregor GR, Thompson CB, Korsmeyer SJ. 2001. Proapoptotic BAX and BAK: A requisite gateway to mitochondrial dysfunction and death. Science 292:727–730.
Wilson BC, Olivo M, Singh G. 1997. Subcellular localization of Photofrin and aminolevulinic acid and photodynamic cross-resistance *in vitro* in radiation-induced fibrosarcoma cells sensitive or resistant to Photofrin-mediated photodynamic therapy. Photochem Photobiol 65:166–176.
Wolter KG, Hsu YT, Smith CL, Nechushtan A, Xi XG, Youle RJ. 1997. Movement of Bax from the cytosol to mitochondria during apoptosis. J Cell Biol 139:1281–1292.
Wu Y, Xing D, Luo S, Tang Y, Chen Q. 2006a. Detection of caspase-3 activation in single cells by fluorescence resonance energy transfer during photodynamic therapy induced apoptosis. Cancer Lett 235:239–247.
Wu Y, Xing D, Chen WR. 2006b. Single cell FRET imaging for determination of pathway of tumor cell apoptosis induced by Photofrin-PDT. Cell Cycle 5:729–734.
Youle RJ, Karbowski M. 2005. Mitochondrial fission in apoptosis. Nat Rev Mol Cell Biol 6:657–663.
Youle RJ, Strasser A. 2008. The BCL-2 protein family: Opposing activities that mediate cell death. Nat Rev Mol Cell Biol 9:47–59.
Yoon Y, Pitts KR, McNiven MK. 2001. Mammalian dynamin-like protein DLP1 tubulates membranes. Mol Biol Cell 12:2894–2905.